

A vector logistic dynamical approach to epidemic evolution on interacting social-contact and production-capacity graphs.*

Jan B. Broekaert¹[0000-0002-4039-8514] and
 Davide La Torre¹[0000-0003-2776-0037]

AI Institute for Business, SKEMA Business School, Sofia Antipolis, France
 jan.broekaert@skema.edu, davide.latorre@skema.edu
<https://www.skema.edu/faculty-and-research/artificial-intelligence>

Abstract. Population inhomogeneity, in the variation of the individual social contact networks and the individual infectious-recovery rates, renders the dynamics of infectious disease spreading uncertain. As a consequence the overlaying economical production network with its proper collaboration components is to extent impacted unpredictably. Our model proposes a *vector logistic* dynamical approach to SIS dynamics in a social contact network interacting with its economic capacity network. The probabilistic interpretation of the graph state in the vector logistic description provides a method to assess the effect of mean and variance of the infected on the production capacity and allows the strategic planning of social connectivity regulation. The impact of the epidemic mean effects and fluctuations on the production capacity is assessed according *cumulative*, *majority* and *fragility* proxy measures.

Keywords: SIS dynamics · vector logistic equation · social graph · production capacity.

1 Context and rationale

Compartmental epidemic models, starting with Kermack and McKendrick [11] and various elaborations reviewed by Hethcote [9], provide a simplified description of the epidemic evolution through transitions between a number of categories in a population, mainly the Susceptible, Infected, and Receptive (‘Recovered’ or ‘Removed’) - and in further model extensions, the Exposed (latency of onset), the Deceased (change of population size) and the Maternal (immunity protection from birth), see e.g. [6]. The aspects of socio-spatial distribution of individuals - in terms of inhomogeneity of both the infection-recovery rates and the connectivity of each individual, and the *stochastic* nature of transition events require an extension of the basic compartmental approach. To encompass the effect of socio-spatial structure of the population in the endemic progression, and to cover the resulting fluctuations, complex graph topologies have been implemented [10,16],

* Advances in Production Management Systems - APMS 2021 conference paper

and reformulated as the bond percolation problem [14]. Specific graph topologies have been related to epidemic extinction time by Ganesh et al. [7] and the resilience of epidemics related to the diameter of the underlying network (e.g. in the network structures of Facebook, the Internet, Social networks) by Lu et al. [12]

Non-deterministic epidemic models including the effects of fluctuations are based on stochastic diffusion equations, by approximating the continuous time Markov chain model [1], by matching as an epidemic model with multiple hosts [13], or by parameter perturbation [8].

Instead, our model develops a description of the epidemic dynamics immediately at the level of intrinsic infection probability, similar to probabilistic Markov or ‘quantum-like’ system descriptions, e.g. [5,18,3]. In our model we describe the interaction of two networks: the social contact network, as the graph union of all individual ‘ego’ contact networks, and the production capacity network as the graph union of all production clusters. The nodes spanning both encompassing networks, $\mathcal{G}_A(V, E_A)$ and $\mathcal{G}_B(V, E_B)$, are the individuals of the considered population (filtered for professional activity in the production capacity graph).

We must take care to distinguish the concept of sub graphs - the connected components which do not share any edge with other such components, either in $\mathcal{G}_A(V, E_A)$ or $\mathcal{G}_B(V, E_B)$, and the interacting graphs which are (two) separate implementations - or layers - of functional relations on the same population. While the existence of connected components, or sub graphs, in the social contact network $\mathcal{G}_A(V, E_A)$ has an effect on the dynamics of infectious disease spreading, and can be indirectly influenced by regulated restriction on the degree of social connectivity, such an intervention is not applicable in the economic capacity network. The connected components of the production capacity graph remain fixed over time, since these components represent the economic capacity units of individual businesses, enterprises or service systems. It has been shown that, for interdependent networks failures in one network can percolate in another network on which its optimal performance depends [4]. In this manner, the interaction of the social graph with the production graph will allow an assessment of the production capacity attrition and will allow an analysis for the possible planning of regulatory intervention in the social contact network.

Finally as we have shortly mentioned earlier, in our approach each node of the graph is characterised by its probability of being infected over time, instead of attributing to each node a binary status of “infected” or “not-infected” at each instance of time. The evolution of the node infection probabilities is determined by the N -dimensional *vector logistic* equation. A similar probabilistic infection approach on a graph was proposed by Wang et al. [17], but which applied a Markov-like dynamics (idem, Eq.13) instead. The usage of the vector logistic equation allows i) to regain the limit of the classic scalar logistic equation for SIS dynamics when the social graph nears the complete graph, $\mathcal{G}_A(V, E_A) = \mathcal{K}_N$ with large N , and ii) a probabilistic interpretation of the graph state vectors of the nodes, \mathbf{Y} , in the unit N -hypercube $[0, 1]^N$. This approach hence allows the expression of any infection related expectation quantity $\langle \mathbf{f} \rangle_t = E_t(\mathbf{f}) = \sum_i Y_i(t) f_i$.

2 Probabilistic SIS-dynamic on social contact graphs

In the compartmentalised SIS-model the dynamics of the infected fraction i , is determined by the recovery rate δ over the infected fraction, and the infection rate β on the product of the susceptible, s , and infected, i , fractions:

$$\dot{i} = -\delta i + \beta(1-i)i, \quad (1)$$

where $1-i(t) = s(t)$. Two stationary solutions can occur $i_1^* = 0$ and $i_2^* = 1 - \delta/\beta$ (the latter when $\delta < \beta$). In our model, the possible interaction between the individuals - represented by nodes - is controlled by the adjacency matrix A of the graph $\mathcal{G}_A(V, E_A)$, $|V| = N$, $E_A \subset V^2$, representing the social contact network. While the specific realisation of the adjacency matrix in the true social contact network remains unknown, a number of parameters can be estimated or assumed [2]. Some of its properties like the average degree can be regulated as an optimisation parameter, e.g. corresponding with the restricted number of contacts that are allowed in a personal ‘social bubble’ or ‘support circle’.

In order to retain a detailed description at the level of individual agents and to assess fluctuations over the network, a probability based infection-recovery model is constructed on a network. In this approach, a probability Y_i of being infected is attributed to each node i . Conform to the interaction effect by ‘contact’, we express the exposure of a node i by the product of its proper receptive capacity $1 - Y_i$ and the infective capacity Y_j of an adjacent node j , i.e. $A_{ij} = 1$, weighted by infection rate β_j and moderated by a normalisation factor of the inverse of the node’s degree d_i^{-1} .

$$\dot{Y}_i = -\delta_i Y_i + d_i^{-1}(1 - Y_i) \sum_j A_{ij} \beta_j Y_j \quad (2)$$

The dynamical equation of the graph state vectors is written in vector notation by using $\boldsymbol{\delta}$ both for the variable recovery rate vector and likewise $\boldsymbol{\beta}$ for the variable infection rate vector and for the state vector \mathbf{Y} . We further need the Hadamard product symbol, \circ , to express the *elementwise* multiplication of factors:

$$\dot{\mathbf{Y}} = -\boldsymbol{\delta} \circ \mathbf{Y} + (\mathbf{1} - \mathbf{Y}) \circ \mathbf{d}^{-1} \circ A (\boldsymbol{\beta} \circ \mathbf{Y}) \quad (3)$$

this notation requires that for an isolated node the apparent division ‘0/0’ occurring in $A(\boldsymbol{\beta} \circ \mathbf{Y})/\mathbf{d}$ is effectively set equal to 0.

This vector differential equation differs from (the linear form of) the generalized Lotka-Volterra equation by a term proportional to $A\mathbf{Y}$, and from the Replicator equation by its additionally lacking a third order term $\mathbf{Y} \circ (\mathbf{Y}^T A \mathbf{Y})$, and having a first-order term in \mathbf{Y} instead. Essentially the equation differs from these two typical dynamical systems by the first order derivative of the state **not** being a Hadamard product with the state itself. In order to attribute a probabilistic interpretation to the magnitudes Y_i , two observations are made,

- when $Y_i = 1$, the component Y_i decays over time at rate δ_i ,

- when $Y_i = 0$, the component Y_i grows at rate $1/d_i \mathbf{A}_{ij}(\boldsymbol{\beta} \circ \mathbf{Y})^j$, which is non-negative.

With an initial state $0 \leq \mathbf{Y}_0 \leq 1$ at $t = 0$, the component values of \mathbf{Y}_t remain contained in the $[0, 1]$ range and hence can be considered as event probabilities (for infection) assigned to the respective nodes of the graph $\mathcal{G}(V, E)$. The state space of the vectors \mathbf{Y} is the unit N-hypercube $[0, 1]^N$, allowing each node an infection probability between 0 and 1. We recall that in contrast, in the Replicator system the corresponding state vector \mathbf{Y} would remain on the simplex, $\sum_{i=1}^N Y_i = 1$, see e.g. Ohtsuki et al. [15], and in the case of the generalized Lotka-Volterra equation the solution is unconstrained $Y \in \mathbb{R}^{+N}$.

It can be easily shown that the vector logistic system reduces to the standard compartmentalised SIS equation when the graph is complete $\mathcal{G}(V, E) = K_N$ (all nodes have grade $N - 1$), and the recovery and infection rates are considered constant over the graph. With $i = \frac{1}{N} \sum_j Y_j$ and $A\mathbf{Y} = N\mathbf{i} - \mathbf{Y}$, where $\mathbf{i} = i\mathbf{1}$, we recover the SIS equation, Eq. (1), after component-wise summation of Eq. (2), and division by N .

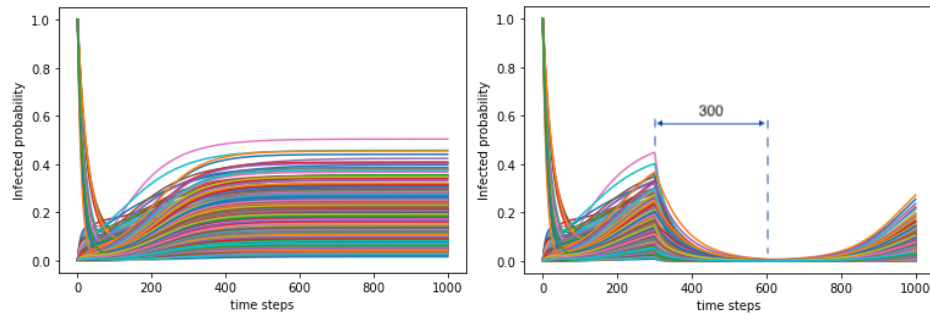


Fig. 1. An illustrative epidemic evolution on a random social contact graph $\mathcal{G}_A(V, E_A)$ with number of nodes $N = 1000$, number of initially infected nodes $init_infected = 10$, and average social connectivity $N_connect_A = 40$ (left). The variable infection rate $\beta = 0.6(\text{SD}0.2)$, and the variable recovery rate $\delta = 0.55(\text{SD}0.2)$. During the confinement, the degree-inducing social contacts parameter is reduced to $N_confinement_A = 20$. The confinement period, Δt_{conf} , starts at time 300 and is held on for 300 time steps (right).

Finally, with the factor of the social contact graph included in the SIS dynamics, Eq. (3), it is now possible to study the effect on the epidemic progression by changes in the graph structure, see Fig. (2). In particular the effect of diminishing the social person-person contacts by culling edges in $\mathcal{G}(V, E)$, see Fig. 2, while maintaining the degree vector \mathbf{d} , allows the dynamical description of confinement efforts in diminishing the epidemic progression.

Concurrently the cost impact from production capacity attrition in the interacting economic graph can be monitored. In the next section, Sec. 3, we define graph-based objective functions for economic capacity. In relation to the social graph, a social cost can be defined proportional to the contact restrictions and the duration of the confinement, see Fig. 1, through the quantity

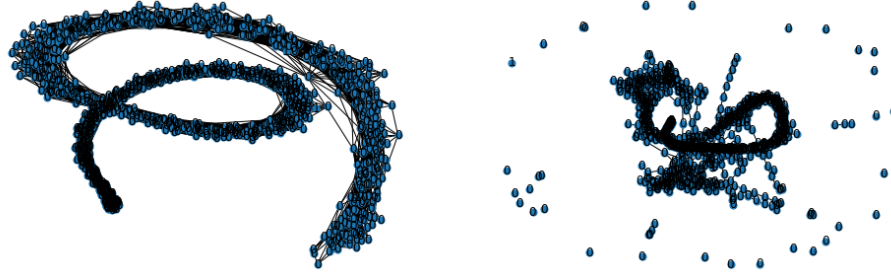


Fig. 2. An unconstrained artificial social contact graph (left) and its confinement rendition (right). In the unconstrained graph ($N = 1000$, $skew = 4$, $N_{connect_A} = 40$) the mean degree is 25.82, the mean cluster coefficient is 0.28, and the graph has 4 connected components. In the confined graph ($N = 1000$, $skew = 4$, $N_{confinement_A} = 20$) the mean degree has decreased to 8.04, with 88 connected components resulting.

$(N_{connect_A} - N_{confinement_A})\Delta t_{conf}$. The epidemic health cost can be defined proportional to total infection weight on the social graph at each instance of the epidemic through the quantity $\int^T |\mathbf{Y}(t)|_1 dt$.

3 The interacting economic capacity network

In our present development of the interacting graphs model we build partially sorted random graphs to resemble real-world configurations - both in social connectivity and economic networks. In principle there is no restriction on implementing another topology in either of the interacting graphs. Using the partially

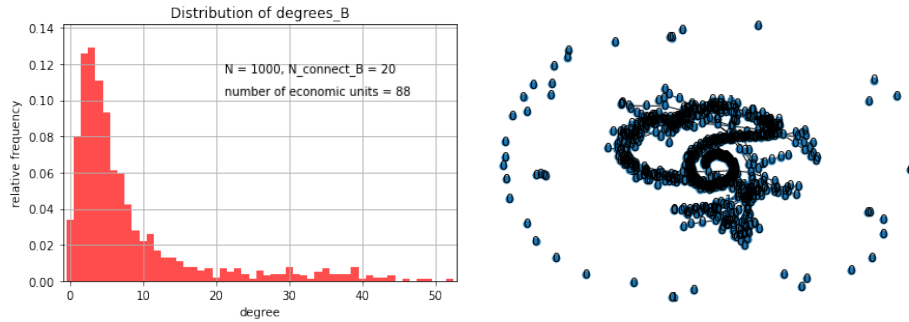


Fig. 3. Construction of the random economic capacity graph $\mathcal{G}_B(V, E_B)$ (right) interacting with the social contact graph $\mathcal{G}_A(V, E_A)$, Fig. 2. The economic capacity network inherits the nodes V_A of the social contact graph ($N = 1000$), and is parametrized by average connectivity parameter $N_{connect_B} = 20$ to obtain a number of economic capacity units $n_B = 88$ (left).

sorted random implementation for the economic capacity graph, the Laplace matrix associated to the adjacency matrix B of $\mathcal{G}_B(V, E_B)$ is used to identify the

independent economic units, n_B in number. The eigenvectors of the Laplace matrix $\delta_B \circ \mathbf{1} - B$ with 0-eigenvalue correspond to the connected components of the graph. With E_{B_i} the eigenvector of the i -th economic capacity unit, a number of proxy measures for production capacity can be formulated. At each instance of time, the epidemic evolution on the social contact graph $\mathcal{G}_A(V, E_A)$ provides the infected states of all individuals $\mathbf{Y}(t)$. Using a threshold value θ in the range $[0, 1]$ on the infection probability, the drop-out of active individuals can be assessed at all moment of time. Then using the *ceiling* function; $Y_{act}(t) = |\text{ceil}(\mathbf{Y}(t) < \theta)|_1$, is the number of healthy individuals. Similarly to identify the active individuals of the i -th graph component in optimal situation (no drop-out), we define its binary vector $\mathbf{W}_{B_i} = \text{ceil}(E_{B_i})$. The epidemic repercussions on each of the economic units can be assessed according the nature of the dependence of the economic output on the active nodes in the economic unit:

1. *cumulative metrics*

The drop-out of individuals on the i -th economic component can impact the capacity of the unit proportionally:

$$c_{cum.i} = \mathbf{Y}_{act}(t)^T \cdot \mathbf{W}_{B_i}$$

The total *cumulative* capacity of the full economic network $\mathcal{G}_B(V, E_B)$ is given by $C_{cum_B} = \sum_{i=1}^{n_B} c_{cum.i}$.

2. *majority*

The drop-out of individuals on the i -th economic component can impact the integral capacity of the unit by majority support (or other tip-over value):

$$c_{maj_i} = \text{ceil} \left(\frac{|\mathbf{Y}_{act}(t)^T \circ \mathbf{W}_{B_i}|_1}{|\mathbf{W}_{B_i}|_1} \geq .5 \right)$$

The total *majority* capacity of the full economic network $\mathcal{G}_B(V, E_B)$ is given by $C_{maj_B} = \sum_{i=1}^{n_B} c_{maj.i}$.

3. *fragility*

The drop-out of each single individual of the i -th economic component impacts the integral capacity of the unit:

$$c_{frag_i} = \prod_{j=1}^{|\mathbf{W}_{B_i}|} (\mathbf{Y}_{act}(t) \cap \mathbf{W}_{B_i})_j$$

where we select by intersection strictly the components corresponding to the i -th economic component, and multiply each. The total *fragile* capacity of the full economic network $\mathcal{G}_B(V, E_B)$ is given by $C_{frag_B} = \sum_{i=1}^{n_B} c_{frag_i}$.

With the objective functions for economic capacity defined, and a standard expression for social cost of confinement proportional to $(N_{connect_A} - N_{confinement_A}) \Delta t_{conf}$ and a health cost proportional to $\int^T |\mathbf{Y}(t)|_1 dt$, an optimization procedure based on parameters $N_{confinement_A}$ and Δt_{conf} can be developed.

4 Implementation and simulation results

A partially sorted random-based social contact graph was implemented to reflect more realistic aspects of true person-person networks as reconstructed by e.g. Barrett et al. [2]. In particular the adjacency matrix, A , of a graph on $N=1000$ nodes was designed and parametrized ($skew, N_connect_A$) to qualitatively approximate the degrees distribution, cluster coefficient distribution and template graph distribution in the communities of Los Angeles, New York City and Seattle [2]. The upper triangular matrix (diag= $+1$) of an ascending in-row sorted random $N \times N$ matrix in the range $[0, 1]$ was used to construct a symmetric matrix A_sorted with the max values in the upper triangle aligning the main 0-diagonal. Its unsorted counterpart A_base was retro-fitted by shuffling the row entries right of the main diagonal and restoring symmetry by fitting the lower triangle with the transposed upper triangle matrix. Clearly the sorted proto-adjacency matrix A_sorted (still with scalars in the range $[0, 1]$) amasses long linkage and fosters clique formation along the diagonal. In order to tweak this architecture, a parameter $skew$ was used to gradually mix in the sorting effect on the random graph. Finally a degree-indicative connectivity parameter, $N_connect_A$, was used to fix the threshold $(N - N_connect_A)/N$ for binary adjacency in A :

$$A_fin = A_sorted + (A_base - A_sorted)/skew$$

$$A = (A_fin \geq (N - N_connect_A)/N) \times 1$$

A number of parameter configurations were repeatedly tested to show for $N = 1000$ that $skew = 4$ and $N_connect_A = 40$ lead to an average degree of approximately 26 and an average cluster coefficient of .27 approximately, and qualitatively approximates the degrees distribution and cluster coefficient distribution of true social contact graphs [2]. The cluster coefficient distribution can be easily obtained from the adjacency matrix. It is given by the number of unique triangular walks from node ν_i over the number of contacts in the neighbour sub-graph had it formed a clique: $cc(\nu_i) = \frac{A_{ii}^3/2}{\binom{d_i}{2}}$. This sorting and tweaking procedure to construct the artificial social contact network moreover produces cycle and clique template graphs of low degrees. E.g., the particular graph $\mathcal{G}_A(V, E_A)$ in Fig. 2, counts 111216 of 3-cliques, and 1082464 of 4-cliques. The number of 3-cycli is of course the same as the number 3-cliques, and the number of 4-cycli is 4831030.

The node-based perspective of the SIS-dynamics was further deployed to randomly attribute individual infection and recovery rates along a lognormal distribution. In particular for the graph $\mathcal{G}_A(V, E_A)$ in Fig. 2, with infection rate β of mean $\log(0.6)$ and 0.2 standard deviation and, recovery rate δ of mean $\log(0.55)$ and 0.2 standard deviation, see Fig. 5.

We reckon that the social planner impacts the social contact graph during the confinement period by bringing about the degree-indicative connectivity param-

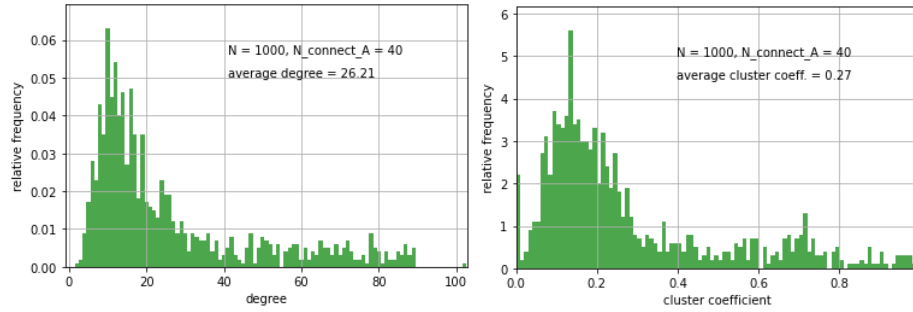


Fig. 4. The degree distribution of the random artificial social contact graph $\mathcal{G}_A(V, E_A)$ (left), and the corresponding cluster coefficient distribution (right).

eter to a smaller value $N_confinement_A$. This parameter most closely reflects the restriction on the number of contacts that are allowed in a personal social bubble during confinement.

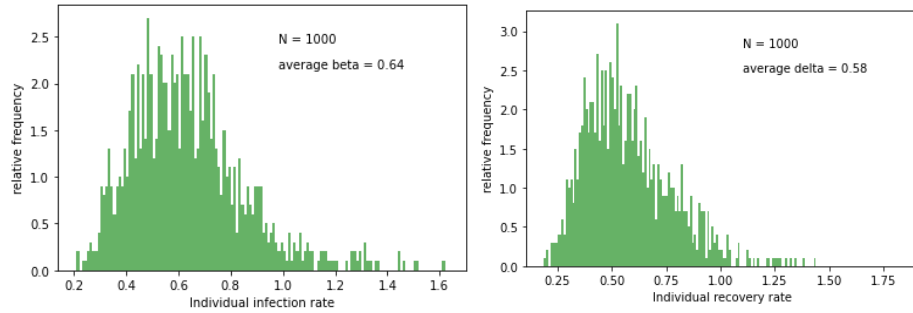


Fig. 5. The lognormal random distributions of infection rate (left) and recovery rate (right) in the random artificial social contact graph $\mathcal{G}_A(V, E_A)$.

Finally the multiplicative structure of the right-hand side of the logistic vector first-order differential equation, Eq. 3,

$$\dot{\mathbf{Y}} = \mathbf{f}(\mathbf{Y})\mathbf{Y}$$

allows a standard solution approach. From the initial state $\mathbf{Y}(0) = \mathbf{Y}_0$ an incrementally updated solution is obtained. The solutions for the full time-range are obtained by the iterated multiplication with a propagator kernel adapted to the previous state;

$$\mathbf{Y}_{t+1} = (\mathbf{1} + \mathbf{f}(\mathbf{Y}_t)dt) \mathbf{Y}_t.$$

In the illustrative epidemic evolution on $\mathcal{G}_A(V, E_A)$, Fig. 1, the initial state was randomly seeded with $init_infected = 10$ nodes. The evolution of the state

vector \mathbf{Y} over the full time range was obtained using time increment $dt = 0.1$ for a total number of time $steps = 1000$. At the start of the confinement period the propagator kernel is adapted to the reduced adjacency $A_{confinned}$ - with original degrees retained - and applied for next 300 time steps. After the confinement period the original multiplicative kernel based on A is resumed.

5 Discussion and conclusion

We explored the possibilities of the vector logistic equation on a social contact graph for the description of contagious disease progression and the description of the possible economic impact of sanitary measures of contact regulation. Our main effort focused on the framing of a graph-based probabilistic SIS-dynamical approach through the vector logistic equation, and constructing interactions with an economic capacity graph. A method of partial-sorting based method was found to implement a social contact graph which resembles more closely some properties of true person-person contact graphs.

In real world scenarios the property of social contact is graded. In our present approach the individual's binary adjacencies A_{ij} are only attenuated by the neighbour's proper infection rate β_j . More realistically this term should include a parameter to express the contact *intensity* dependent on each respective contact, i.e. by an infection matrix β_{ij} (e.g. related to the time of mutual exposure). Future developments of the graph-based vector logistic dynamics for disease spreading and its economic impact will include development of optimal operational control measures for cost and, refinement of the contamination structure.

Acknowledgements

The authors thank the anonymous referees for suggestions on the reciprocal interaction of the economic graph into the social graph.

References

1. Allen, E.: Modeling with Itô Stochastic Differential Equations. Springer-Verlag The Netherlands (2007)
2. Barrett, C.L., Beckman, R.J., Khan, M., Kumar, V.S.A., Marathe, M.V., Stretz, P.E., Dutta, T., Lewis, B.: Generation and analysis of large synthetic social contact networks. In: Proceedings of the 2009 Winter Simulation Conference (WSC). pp. 1003–1014 (2009). <https://doi.org/10.1109/WSC.2009.5429425>
3. Broekaert, J., Busemeyer, J., Pothos, E.: The disjunction effect in two-stage simulated gambles. an experimental study and comparison of a heuristic logistic, markov and quantum-like model. *Cognitive Psychology* **117**, 101262 (2020). <https://doi.org/https://doi.org/10.1016/j.cogpsych.2019.101262>, <https://www.sciencedirect.com/science/article/pii/S001002851930252X>
4. Buldyrev, S., Parshani, R., Paul, G., Stanley, H., Havlin, S.: Catastrophic cascade of failures in interdependent networks. *Nature* **464**, 1025–1028 (2010). <https://doi.org/10.1038/nature08932>

5. Busemeyer, J., Bruza, P.: Quantum models of cognition and decision. Cambridge, UK: Cambridge University Press (2012)
6. Choisy, M., Guégan, J.F., Rohani, P.: Mathematical modeling of infectious diseases dynamics. *Encyclopedia of Infectious Diseases: Modern Methodologies* (2007)
7. Ganesh, A., Massoulié, L., Towsley, D.: The effect of network topology on the spread of epidemics. In: *Proceedings IEEE 24th Annual Joint Conference of the IEEE Computer and Communications Societies*. vol. 2, pp. 1455–1466 vol. 2 (2005). <https://doi.org/10.1109/INFCOM.2005.1498374>
8. Gray, A., Greenhalch, D., Hu, L., Mao, X., Pan, J.: A stochastic differential equation sis epidemic model. *SIAM Journal on Applied Mathematics* **71**(3), 876–902 (2011)
9. Hethcote, H.: The mathematics of infectious diseases. *SIAM Review* **42**(4), 599–653 (2000). <https://doi.org/10.1137/S0036144500371907>
10. Keeling, M.J., Eames, K.T.: Networks and epidemic models. *Journal of The Royal Society Interface* **2**(4), 295–307 (2005). <https://doi.org/10.1098/rsif.2005.0051>
11. Kermack, W., McKendrick, A.: A contribution to the mathematical theory of epidemics. *Proceedings of the Royal Society of London series A* **115**(772), 700–721 (1927)
12. Lu, D., Yang, S., Zhang, J., Wang, H., Li, D.: Resilience of epidemics for sis model on networks. *Chaos* **27**(083105) (2017). <https://doi.org/10.1063/1.4997177>
13. McCormack, R., Allen, L.: Stochastic sis and sir multihost epidemic models. *Proceedings of the Conference on Differential and Difference Equations and Applications* pp. 775–78 (2006)
14. Newman, M.E.J.: Spread of epidemic disease on networks. *Phys. Rev. E* **66**, 016128 (Jul 2002). <https://doi.org/10.1103/PhysRevE.66.016128>
15. Ohtsuki, H., Nowak, M.A.: The replicator equation on graphs. *Journal of Theoretical Biology* **243**(1), 86–97 (2006). <https://doi.org/https://doi.org/10.1016/j.jtbi.2006.06.004>, <https://www.sciencedirect.com/science/article/pii/S0022519306002426>
16. Tao, Z., Zhongqian, F., Binghong, W.: Epidemic dynamics on complex networks. *Progress in Natural Science* **16**(5), 452–457 (2006). <https://doi.org/10.1080/10020070612330019>
17. Wang, Y., Chakrabarti, D., Wang, C., Faloutsos, C.: Epidemic spreading in real networks: an eigenvalue viewpoint. In: *22nd International Symposium on Reliable Distributed Systems, 2003. Proceedings*. pp. 25–34 (2003). <https://doi.org/10.1109/RELDIS.2003.1238052>
18. Wang, Z., Busemeyer, J., Atmanspacher, H., Pothos, E.: The potential of using quantum theory to build models of cognition. *Topics in Cognitive Science* **5**, 672–688 (2013). <https://doi.org/10.1111/tops.12043>